CHEMCOMM
Communication
www.rsc.org/chemcomm

In situ formation of gold nanoparticles within functionalised ordered mesoporous silica *via* an organometallic 'chimie douce' approach†

Yannick Guari,[a] Chloé Thieuleux,[a] Ahmad Mehdi,[a] Catherine Reyé,[a] Robert J. P. Corriu,*[a] Silvia Gomez-Gallardo,[b] Karine Philippot,[b] Bruno Chaudret*[b] and Roger Dutartre[c]

[a] *Laboratoire de Chimie Moléculaire et Organisation du Solide, UMR 5637 CNRS, Université de Montpellier II, Sciences et techniques du Languedoc, Place E. Bataillon, F-34095 Montpellier Cédex 5, France. E-mail: reye@crit.univ-montp2.fr*

[b] *Laboratoire de Chimie de Coordination du CNRS, 205, route de Narbonne, F-31077 Toulouse Cédex 04, France. E-mail: chaudret@lcc-toulouse.fr*

[c] *Laboratoire des Agrégats Moléculaires et des Matériaux Inorganiques, UMR 5072 CNRS, Université de Montpellier II, Sciences et techniques du Languedoc, Place E. Bataillon, F-34095 Montpellier Cédex 5, France*

Received (in Cambridge, UK) 20th March 2001, Accepted 5th June 2001
First published as an Advance Article on the web 6th July 2001

Functionalized SBA-15 type materials containing mercaptopropyl groups have been used for controlling the growth of gold(0) nanoparticles from $HAuCl_4$ or AuCl(THT) which were chemically complexed within the channels prior to mild chemical reduction.

Metal particles in the nanosize range represent a transition between the molecular and solid states and are therefore of great interest due to their unique properties attributed to quantum confinement or surface effects.[1] Thus, selective synthesis of such nanomaterials with well-defined size[2] and their dispersion in an insulator like SiO_2 is a significant challenge.[3] One approach to obtain such materials consists of using the regular channels of hexagonal mesoporous silica[4] as matrices either for the inclusion of already prepared metal particles[5] or for controlling the growth of metal particles. Such matrices should give rise to composite materials organised at the nano- and the mesoscopic length scales. Thus, the ordered mesoporous silica MCM-41,[6–10] MCM-48,[11] and FSM-16[12] materials have been used as matrices for the growth of mono-[7–12] or bimetallic[6] transition metal nanoparticles. The general procedure was to generate the nanoparticles by calcination of the metallic precursor onto the support. The final nanoparticle size is controlled by the pore size but depends also on the calcination temperature. Furthermore, outer pores growth of nanoparticles is a major frequently encountered drawback of the impregnation/calcination method. This problem has been circumvented by suspending the previously impregnated material in deionised water in order to allow complete migration of the metal salt within the pores[9] or by adding the metal salt during the preparation of the material.[10] Here, we describe a new methodology based on the chemical control of the growth of nanoparticles from organometallic precursors previously reported.[13] The precursor is chemically complexed within the channels of functionalised mesoporous silica[14] and the metal nanoparticles growth is achieved by mild chemical reduction which makes the final particle size only dependent of the pore size on the matrix used.

Materials $HS(CH_2)_3SiO_{1.5}/xSiO_2$ **1** (with $\mathbf{1_a}$: $x = 9$, $\mathbf{1_b}$: $x = 19$) were elaborated by the co-condensation route of 3-mercaptopropyltrimethoxysilane (MPTMS) with tetraethoxysilane (TEOS) in the presence of Pluronic 123 [$PEO_{20}PPO_{70}PEO_{20}$ with PEO = poly(ethylene oxide) and PPO = poly(propylene oxide)] as structure directing agent in acidic media.[15] After extraction of the surfactant by using a Soxhlet apparatus, the materials were vacuum dried at 120 °C.

^{29}Si MAS NMR spectroscopy showed resonances for siloxane (Q^n) and organosiloxane (T^n) centres with a predominance of T^3 compared to T^2 or T^1 centres indicative of extensive condensation of the organic moiety in the wall structure. The solid state ^{13}C CP MAS NMR spectra show signals at δ 27 (C1, C2) in addition to a slightly shifted downfield CH_2–(Si) (C3) signal at δ 11 for the $–(CH_2)_3SH$ moiety. This confirms the presence of mercaptopropyl groups anchored to the pore walls. Furthermore, IR spectra of $\mathbf{1_a}$ (x = 9) display a characteristic S–H stretching vibration of low intensity at 2575 cm^{-1}. High values for the BET surface areas were obtained (Table S1†). The BJH pore size distribution was calculated from adsorption and desorption branches (53/46 Å for $\mathbf{1_a}$ and 71/61 Å for $\mathbf{1_b}$). These values show a significant decrease with increasing the content of thiol groups on the channel surface (Table S1†). The low angle X-ray diffraction (XRD) patterns of the materials show the (100) reflection while higher order (110) and (200) reflections were not well observed.[15]

Anchoring of gold within materials **1** was performed by using two gold precursors with a similar strategy (Scheme 1). The protocols used were based on procedures affording gold(0) nanoparticles in solution.[16] Path A: hydrogenotetrachloroaur-

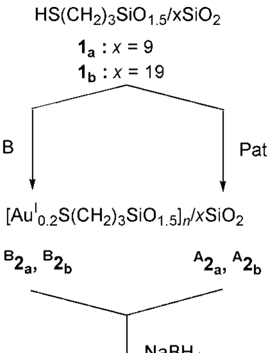

Scheme 1 Preparation of the gold(0) nanoparticle-containing materials. *Reagents and conditions*: path A: i, $HAuCl_4·3H_2O$; ii, $HOC(CO_2Na)(CH_2CO_2Na)_2$. Path B: i, AuCl(THT); ii, Na(acac); H_2O.

---

† Electronic supplementary information (ESI) available: Table S1: Physical properties of ordered mesoporous materials. Fig. S1: Nitrogen adsorption/desorption isotherms of $\mathbf{1_b}$, $^B\mathbf{2_b}$ and $^B\mathbf{3_b}$ and pore size distributions. Fig. S2: Low angle XRD patterns of $\mathbf{1_b}$, $^B\mathbf{2_b}$ and $^B\mathbf{3_b}$ Fig. S3: UV–VIS spectrum of $^B\mathbf{3_b}$. Fig. S4: High angle XRD pattern of $^A\mathbf{3_a}$. Fig. S5: TEM image of $^A\mathbf{3_a}$. Fig. S6 TEM image of $^B\mathbf{3_b}$. See http://www.rsc.org/suppdata/cc/b1/b102575a/

ate(III) hydrate ($HAuCl_4 \cdot 3H_2O$) was added to a suspension of the material in water heated under reflux and allowed to stir until the yellowish solution colour was transferred onto the solid. Then, sodium citrate [$HOC(CO_2Na)(CH_2CO_2Na)_2$] was added. This is the well known Turkevitch method which affords in solution particles of mean size centred near 12 nm. Using this procedure it will therefore be easy to discriminate between nanoparticle growth inside or outside the channels of the mesoporous material previously prepared. Path B: chloro(thiophene)gold(I) [AuCl(THT)] was added at 60 °C to a suspension of the material in THF followed by addition of sodium acetylacetonate hydrate [$Na(acac) \cdot H_2O$]. This procedure is expected to be milder and to lead to a more homogeneous system.

The presence of gold in the expected quantities for the resulting materials **2** was established by elemental analysis. The decrease in BET surface area as well as the decrease in pore volume are consistent with pore filling (Table S1†).

In all cases, it was observed for the X-ray diffractograms that when comparing the results on empty materials **1** and composite materials **2**, the intensity of the reflections was reduced in the latter case. This provides a confirmation of the pore filling of the host material, which reduces the scattering contrast between the pores and the walls of the materials.[17] For materials **2**, absence of plasmon band absorbances in the UV–VIS spectra or of diffraction peaks in the X-ray diffractograms (their presence being characteristics of gold(0) nanoparticles-containing materials) were observed. TEM images show weakly contrasted particles with diameter sizes less than 1.5 nm. These particles, the size of which is not dependent on the host material pore size, were attributed to formation of $(–Au^{I}SR–)_n$ polymers.[18] Therefore, the colourless solids **2** obtained at this stage were treated with an ethanolic sodium borohydride ($NaBH_4$) solution at 60 °C. This mild reduction afforded, after 12 h, purple solids **3** for which further decrease in BET surface area and pore volume was observed (Table S1†). Materials **3** exhibit intense plasmon band absorbance at 520 nm indicative of gold(0) nanoparticles. XRD patterns of materials **3** for the high angle region (2θ = 20–70) show broad reflections characteristic of gold(0) nanoparticles. TEM studies clearly show a narrow gold(0) nanoparticle distribution size for materials **3** whatever the pathway followed (A or B) (Fig. S5 and S6†). It is also clear that in both cases the growth of the particles occurs within the channels of the silica matrix since the size of the particles is quite small (centred near 2.5 and 4.5 nm). The size distribution was found to be more narrow *via* path B ($^{\mathbf{B}}\mathbf{3_b}$) than *via* path A ($^{\mathbf{A}}\mathbf{3_b}$) in agreement with the milder conditions needed for the reduction of the gold(I) precursor. In all cases, a good correlation was demonstrated between the pore size values derived from BET and the gold nanoparticles diameter size observed on TEM micrographs when taking into account experimental uncertainties (Fig. 1).

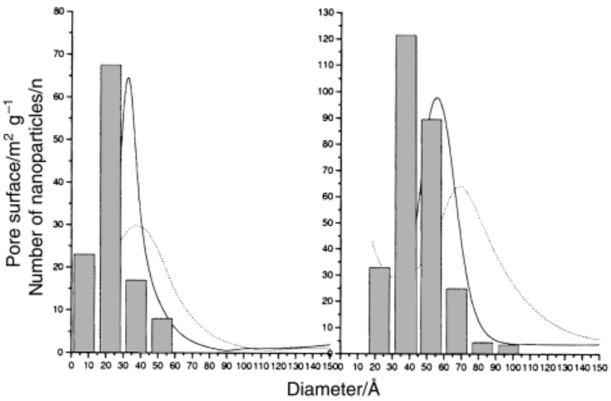

Fig. 1 Correlation between the pore diameter (solid/dotted lines for adsorption/desorption data from N_2 studies) and the gold(0) nanoparticle size (columns) for: left $^{\mathbf{A}}\mathbf{3_a}$, right $^{\mathbf{B}}\mathbf{3_b}$.

In conclusion, two main results are reported in this communication:

(i) The growth of gold nanoparticles can be achieved selectively within the pores of a mesoporous silica previously functionalized with thiol substituents. The nanoparticle growth follows a two step procedure implying first the anchoring of the gold precusors and secondly a chemical reduction.

(ii) This procedure allows a strict control of the size of the particles, which in each experiment, remain smaller than the pore size determined by BET and which furthermore adopt a narrow size distribution. Further work is in progress to explore the scope and limitations of this process.

The authors thank the CNRS and the Université de Montpellier II for financial support. C. T. thanks Air Liquide for a grant. S. G. G. thanks EU, TMR network CLUPOS for a grant.

Notes and references

1 A. P. Alivisatos, *Science*, 1996, **271**, 933; J. Shi, S. Gider, D. Babcock and D. D. Awschalom, *Science*, 1996, **271**, 937.

2 *Clusters and Colloids, from Theory to Applications*, ed. G. Schmid, VCH, Weinheim, 1994.

3 F. Tian and K. J. Klabunde, *New J. Chem.*, 1998, 1275.

4 C. T. Kresge, M. E. Leonowicz, W. J. Roth, J. C. Vartuli and J. S. Beck, *Nature*, 1992, **359**, 710; J. S. Beck, J. C. Vartuli, W. J. Roth, M. E. Leonowicz, C. T. Kresge, K. D. Schmitt, C. T.-W. Chu, D. H. Olsen, E. W. Sheppard, S. B. McCullen, J. B. Higgins and J. L. Schlenker, *J. Am. Chem. Soc.*, 1992, **114**, 10834.

5 D. S. Shephard, T. Maschmeyer, B. F. G. Johnson, J. M. Thomas, G. Sankar, D. Oskaya, W. Zhou, R. D. Oldroyd and R. G. Bell, *Angew. Chem., Int. Ed. Engl.*, 1997, **36**, 2242; D. S. Shephard, T. Maschmeyer, G. Sankar, J. M. Thomas, D. Ozkaya, B. F. G. Johnson, R. Raja, R. D. Olkroyd and R. G. Bell, *Chem. Eur. J.*, 1998, **4**, 1214; R. Raja, G. Sankar, S. Hermans, D. S. Shephard, S. Bromley, J. M. Thomas and B. F. G. Johnson, *Chem. Commun.*, 1999, 1571.

6 D. Ozkaya, W. Zhou, J. M. Thomas, P. Midgley, V. J. Keast and S. Hermans, *Catal. Lett.*, 1999, **60**, 113; F. Schweyer, P. Braunstein, C. Estournès, J. Guille, H. Kessler, H.-L. Paillaud and J. Rosé, *Chem. Commun.*, 2000, 1271.

7 Z. Y. Yuan, S. Q. Liu, T. H. Chen, J. Z. Wang and H. X. Li, *Chem. Commun.*, 1995, 973; Y. Plyuto, J.-M. Berquier, C. Jacquiod and C. Ricolleau, *Chem. Commun.*, 1999, 1653.

8 P. Mukherjee, C. R. Patra, R. Kumar and M. Sastry, *Phys. Chem. Commun.*, 2001, 5.

9 T. Abe, Y. Tachibana, T. Uematsu and M. Iwamoto, *J. Chem. Soc., Chem. Commun.*, 1995, 1617; M. Iwamoto, T. Abe and Y. Tachibana, *J. Mol. Catal. A: Chem.*, 2000, **155**, 143.

10 R. S. Mulukutla, K. Asakura, S. Namba and Y. Iwasawa, *Chem. Commun.*, 1998, 1425.

11 M. Fröba, R. Köhn, G. Bouffaud, O. Richard and G. van Tendeloo, *Chem. Mater.*, 1999, **11**, 2858.

12 A. Fukuoka, M. Osada, T. Shido, S. Inagaki, Y. Fukushima and M. Ichikawa, *Inorg. Chim. Acta.*, 1999, **294**, 281.

13 F. Dassenoy, K. Philippot, T. Ould Ely, C. Amiens, P. Lecante, E. Snoeck, A. Mosset, M.-J. Casanove and B. Chaudret, *New J. Chem.*, 1998, 703; O. Vidoni, K. Philippot, C. Amiens, B. Chaudret, O. Balmes, J. O. Malm, J. O. Bovin, F. Senocq and M.-J. Casanove, *Angew. Chem., Int. Ed.*, 1999, **38**, 3736; C. Pan, F. Dassenoy, M.-J. Casanove, K. Philippot, C. Amiens, P. Lecante, A. Mosset and B. Chaudret, *J. Phys. Chem. B*, 1999, **103**, 10 098; S. Gomez, K. Philippot, V. Collière, B. Chaudret, F. Senocq and P. Lecante, *Chem. Commun.*, 2000, 1945; K. Soulantica, A. Maisonnat, M.-C. Fromen, M.-J. Casanove, P. Lecante and B. Chaudret, *Angew. Chem., Int. Ed.*, 2001, **40**, 448.

14 R. J. P. Corriu, C. Hoarau, A. Mehdi and C. Reyé, *Chem. Commun.*, 2000, 71; R. J. P. Corriu, A. Mehdi and C. Reyé, *C.R. Acad. Sci. Paris, Sér. IIc*, 1999, 35; R. J. P. Corriu, Y. Guari, A. Mehdi, C. Reyé and C. Thieuleux, *Chem. Commun.*, 2001, 763.

15 D. Margolese, J. A. Melero, S. C. Christiansen, B. F. Chmelka and G. D. Stucky, *Chem. Mater.*, 2000, **12**, 2448.

16 J. Turkevitch, P. C. Stevenson and J. Hillier, *Discuss. Faraday Soc.*, 1951, **73**, 55.

17 B. Marler, U. Oberhageman, S. Vortmann and H. Gies, *Microporous Mater.*, 1996, **6**, 375.

18 A. C. Templeton, W. P. Wuelfing and R. W. Murray, *Acc. Chem. Res.*, 2000, **33**, 27.